

CLEO III, A Dectector To Measure Rare B Decays and CP Violation

Sheldon Stone¹

Physics Dept., Syracuse Univ., Syracuse, NY, 13244-1130

Abstract

The symmetric e^+e^- collider CESR is undergoing a series of upgrades allowing for luminosities in excess of $2 \times 10^{33} \text{cm}^{-2} \text{s}^{-1}$. The most important goals of the upgrade are precision measurement of standard model parameters V_{cb} , V_{ub} , V_{td}/V_{ts} , f_{D_s} , and searching for CP violation and standard model violations in rare B decays. A new detector upgrade, called CLEO III, has started which includes a new silicon-wire drift chamber tracking system and a Ring Imaging Cherenkov Detector, RICH, using a LiF radiator and CH_4 -TEA gas based photon detector.

.....
Presented at BEAUTY '95 - 3rd International Workshop on B-Physics at Hadron
Machines Oxford, UK, 10-14 July, 1995

¹Stone@suhep.phy.syr.edu

1 Introduction - B Physics Goals

The CLEO collaboration is in the midst of a detector upgrade, to match the CESR increase in luminosity to $> 2 \times 10^{33} \text{cm}^{-2}\text{s}^{-1}$ and to insure meeting the physics goals described below.

The current extent of knowledge on weak mixing in the quark sector can be shown by plotting constraints in the η and ρ plane given by measurements of the ϵ parameter describing CP violation in K_L^0 decay, and by $B^0 - \bar{B}^0$ mixing and semileptonic $b \rightarrow X\ell\nu$ decays. An analysis of the allowed parameter space is shown in Figure 1 [1]. Overlaid on the figure is a triangle that results from the requirement $V \cdot V^\dagger = 1$, i.e. that the CKM matrix be unitary. Measurements of CP violation in B decays can, in principle, determine each of the angles α , β and γ of this triangle independently.

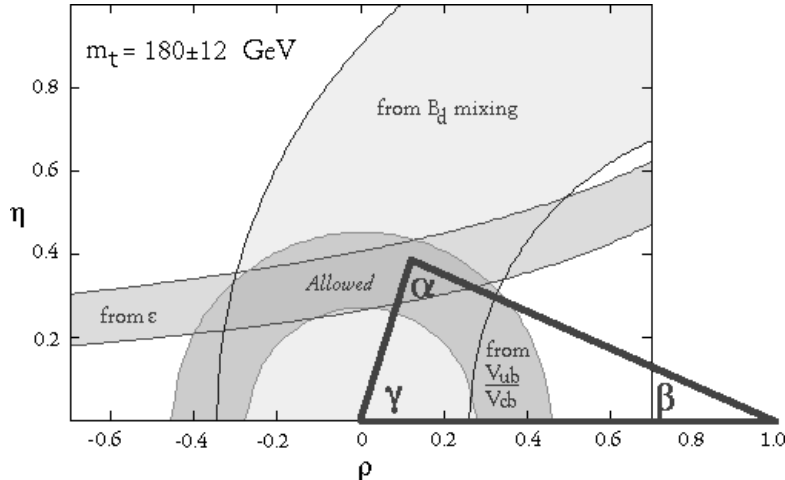


Figure 1: The CKM triangle overlaid upon constraints in the $\rho - \eta$ plane, from measured values of V_{ub}/V_{cb} , $B^0 - \bar{B}^0$ mixing and ϵ in the K^0 system. The allowed region is given by the intersection of the three bands.

There are many measurements to make with CLEO III. Here I will only mention a few of the most important.

- The dominant error in the ϵ band is caused by the uncertainty in V_{cb} . This can be improved, for example, by measuring the rate for $B^- \rightarrow D^{*0}\ell^- \nu$ at maximum four-momentum transfer.
- The error in the V_{ub} band can be decreased by using exclusive semileptonic decays such as $\pi\ell^- \nu$ [2].

- The error on the mixing band comes dominantly from the lack of knowledge of f_B . We can reduce this uncertainty by comparing models with our measurement of f_{D_s} currently $(284 \pm 30 \pm 30 \pm 16)$ MeV [3].
- The ratio V_{td}/V_{ts} may be ascertained by measuring the ratio of the $\rho\gamma/K^*\gamma$ branching ratios [4]. The basic idea here is that the difference in the two final states comes mainly from having V_{ts} in the case of $K^*\gamma$ and V_{td} for $\rho\gamma$. Although it has been argued that other diagrams may contribute to the numerator this would lead to the inequality of $\rho^+\gamma$ and $\rho^-\gamma$ and would therefore be a measurement of direct CP violation. It is also likely that these other diagrams would induce an inequality between neutral and charged ρ final states. In short, this is a very interesting physics area.
- Measure CP violation. We will try and measure the CP violation angle γ using one of two techniques. The first, suggested by Gronau and London, involves measuring the rates for $B^- \rightarrow D^0 K^-$, $\overline{D}^0 K^-$ and $D_{CP}^0 K^-$, and the corresponding rates for B^+ decay. (D_{CP}^0 indicates that the D^0 decays into a CP eigenstate, for example $K^+ K^-$.) The second involves measuring a rates for two-body pseudoscalar decays $\pi^\pm \pi^0$ and $K^\pm \pi^0$ etc...[4]. Other attempts to measure CP violation through rate asymmetries such as differences between $\psi\pi^+$ and $\psi\pi^-$ or even to measure the angle β by using the standard ψK_s mode and the small B motion in our symmetric e^+e^- collider.

2 CESR upgrades

CESR has achieved the highest instantaneous luminosity of any e^+e^- collider, $\approx 2 \times 10^{32} \text{cm}^{-2}\text{s}^{-1}$. However, heavy quark physics is limited by the number of events, so even higher luminosities are desired. The approved CESR upgrade will have luminosity in the range of 2×10^{33} . This is accomplished in two stages. In the first stage there will be 9 “trains” of 3 bunches, and a small horizontal crossing angle, with a goal of 6×10^{32} . This phase is being implemented now. The second stage has 9 trains of 5 bunches, a larger horizontal crossing angle, a smaller β_v^* (≈ 1 cm) requiring a new interaction region and therefore a new inner detector, and superconducting RF cavities.

There is also a future plan being developed, to reach luminosity in excess of 5×10^{33} by using 180 bunches, round beams in the interaction region and a reduced bunch length. This plan would use the same inner detector being built now, which is the subject of the rest of this article.

3 The CLEO III Detector Upgrade

The CLEO II goal was to reconstruct thousands of B mesons using excellent tracking and photon detection and modest particle identification. Although the CLEO II goals have been met, experience with the detector and the desire to meet new physics goals, have uncovered several serious deficiencies. These include the rather thick drift chamber endplate and associated material which seriously compromises photon detection in the endcaps and outer barrel region, and the lack of good quality charged hadron identification² above 750 MeV/c. Furthermore, the electronics and DAQ system will not support the higher interaction rates caused by the increased luminosity. Finally, the inner tracking detector must be replaced because part of the space is necessary for the final focus quadrupoles.

There are several advantages to the detector being upgraded since CESR is a symmetric energy accelerator. It is easier to have a large solid angle coverage than in an asymmetric machine, since less of the phase space goes down the beam pipe. The maximum momentum of a B decay product is 2.8 GeV/c, rather than about 4 GeV/c for an asymmetric machine operating at the $\Upsilon(4S)$. It is also important that we can build upon our existing detector utilizing some of the more expensive parts such as the CsI calorimeter, the magnet and the muon system, all of which have functioned excellently.

The design philosophy of CLEO I was to have excellent tracking and charged particle momentum resolution. Advances in crystal growth techniques, superconducting magnet technology and electronics made it possible to add excellent photon and electron detection in CLEO II [5]. The design philosophy of CLEO III is to maintain the excellent charged particle resolution while sacrificing 20 cm of space for charged particle identification. This is possible because we can add a high precision silicon detector near the beam pipe which can precisely determine angles and then have a low mass drift chamber which can precisely measure transverse momentum. It is important to realize that multiple scattering is the largest source of tracking errors over the entire range of B decay momenta at CESR.

An overview of CLEO III is shown in Fig. 2. There is a four layer silicon detector, followed by a drift chamber with staggered inner section to accommodate the CESR final focus quadrupoles. Radially beyond this is 20 cm space for the barrel particle identification detector. At the ends of the detector are relocated and repackaged CsI calorimeter endcaps with improved performance and provision for mounting the drift chamber and CESR machine components.

²The Drift Chamber dE/dx system does provide $\sim 2\sigma$ K/π separation above 2.3 GeV/c.

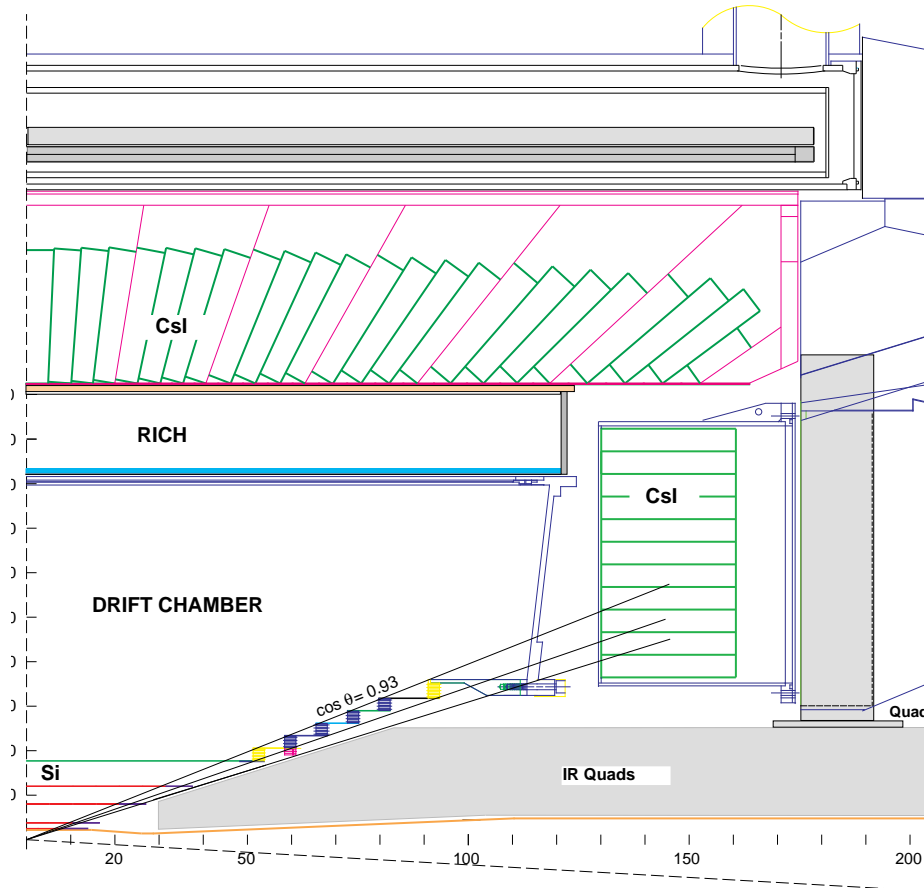


Figure 2: Quarter section of the CLEO III detector.

4 The RICH system

4.1 Introduction

Ring imaging Cherenkov detectors (RICH) are capable of providing excellent identification of charged particles. Several systems have been implemented in hadron beams and e^+e^- collider experiments [6].

The CLEO RICH is based on the ‘proximity focusing’ approach, in which the Cherenkov cone is simply let to expand in a volume filled with ultraviolet transparent gas (the expansion gap) as much as allowed by other spatial constraints, before intersecting the detector surface where the coordinates of the Cherenkov photons are reconstructed. The components of our system are illustrated in Fig. 3. It consists of a LiF radiator, providing U.V. photons, an expansion region, and a photosensitive detector made from a wire proportional chamber containing a CH_4 -TEA gas mixture. The cathode plane is segmented into pads to reconstruct the photon positions.

The design is based on work of the College de France–Strasbourg group,[7]. We are considering a unique geometry for the LiF solid radiator [8], where the light emitting surface is shaped like the edge of a saw blade with the teeth angled at 45° . If we can manufacture

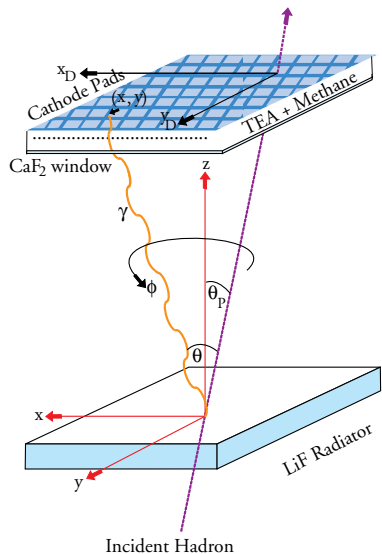


Figure 3: Schematic diagram of LiF-TEA RICH system.

this shape it will produce more photons and achieve better resolution. A fine segmentation of the cathode pad ($\approx 7.5 \times 8 \text{ mm}^2$) is required in order to achieve the spatial resolution needed, which in turn implies a high density of readout electronics.

The angular resolution per detected photon is comprised of several sources. The most important are the chromatic error, which results from the variation of the index of refraction with the wavelength, the emission point error, which results from the lack of knowledge about where the photon is emitted, and the position error in detecting the photon. There is also a small error caused by the inability to resolve some of the overlapping photon cluster. The individual sources of error have been determined by using GEANT. The combined resolution is about 13.5-14 mrad resolution per detected photon independent of the track incident angle. This corresponds to a 3.7 mrad resolution per track. Since the difference in Cherenkov angle between pions and kaons is 12.8 mr at 2.8 GeV/c we expect this system to have at least 3.5 standard deviation separation. However, should it be possible to obtain the sawtooth radiators, the separation will be much better [8].

The device will be constructed with a 30 fold segmentation. The LiF radiators are held in place by an inner carbon fiber cylinder to which they are attached. The back of the cathode boards which constitute the outer side of the MWPC are strengthened by hollow G10 rods which also act as channels for the cooling gas (N_2). The strength has been achieved with great care to minimize the amount of material in the detector, in order to preserve the excellent performance of the electromagnetic CsI calorimeter. The average material thickness is 13% of a radiation length for tracks at normal incidence.

4.2 Readout Electronics

The 230,000 readout channels are distributed over the surface at the outer radius of the detector and are impossible to access routinely. Therefore the readout architecture must feature high parallelism, and extensive testing of active components and connection elements is required in order to insure their reliability. The MWPC detector surface is segmented into 30 modules, which will be divided into 12 subunits each with 640 readout channels. Each of these subunits will communicate via a low mass cable connection with VME cards providing the control signals and receiving the analog or digitized signals as discussed below.

Several considerations affect the design of the individual channel processor. Low noise is an essential feature because the charge probability distribution for the avalanche produced by a single photon is exponential at moderate gains. It should be stressed that it is beneficial to run at low gains to improve the stability of chamber operation. Therefore in order to achieve high efficiency, the noise threshold should be as low as possible. An equivalent noise charge of about 200 electrons is adequate for our purposes. On the other hand, an exponential distribution implies that a high dynamic range is desirable in order to preserve the spatial resolution allowed by charge weighting. Note that charged particles are expected to generate pulses at least 20 times higher than the single photon mean pulse height. In order to improve the robustness of the readout electronics against sparking, a protection circuit constituted by a series resistor and two reverse biased diodes is required in the input stage. Finally it is important to sparsify the information as soon as possible in the processing chain, as the occupancy of this detector is very low and therefore only a small fraction of the readout channels contain useful signals.

There is a preamplifier/shaper VLSI chip developed for solid state detector applications which incorporates many of the features discussed above [2]. A dedicated version of this chip, called VA_RICH, has been developed and will be tested shortly. Its predicted equivalent noise charge is given by:

$$ENC = \sqrt{(73e^- + 12.1 * Ce^-/pF)^2 + (50e^-)^2}, \quad (1)$$

where C is the input capacitance of ≈ 2 pf. The first term corresponds to the noise contribution from the input transistor and the (80 Ω) series resistor used for the input protection and the second to the noise from subsequent stages, small but non negligible because of the lower gain chosen to increase the dynamic range. This device is expected to maintain linear response up to an input charge of 700,000 e^- .

The choice of digitization and sparsification technique has not yet been finalized. Under consideration is the digitization and sparsification at the front end level, using the zero

suppression scheme and the ADC included in the SVX II readout chip [10]. Alternatively we will digitize all the analog output signal and perform the zero suppression afterwards.

4.3 Results from Prototype

We have constructed a prototype of an individual detector module about 1/3 the length of an actual detector module and about the same width. The prototype system is enclosed in a leak tight aluminum box. The expansion gap is 15.7 cm. In this prototype we have used plane 1 cm thick LiF radiators. The chamber geometry is approximately the same as the final design in terms of gap size, wire to cathodes distance and pad sizes. The total number of pads read out is 2016. Pad signals are processed by VA2 preamplifier and shapers [9]. The detector plane is divided into 4 quadrants each of which has 8 VA2 daisy-chained for serial readout.

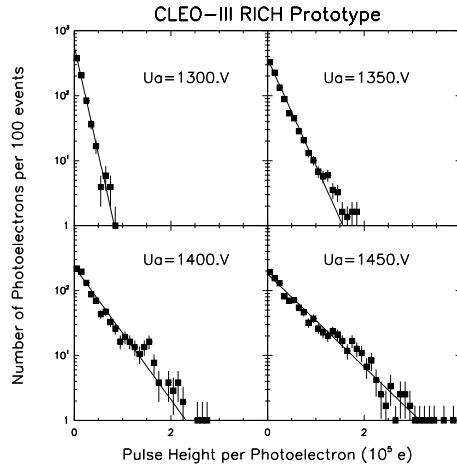


Figure 4: Photon induced avalanche charge distribution at different anode voltages. The voltage on the metallization of the CaF_2 windows is kept at -1350V.

This prototype has been exposed to hardened cosmic rays. Fig. 4 shows the charge distribution of reconstructed photon clusters as a function of the anode wire voltage U_a for several different voltages. Note that the pulse height distribution is consistent with an exponential profile and its mean value increases with U_a , as expected. Fig. 5 shows the excitation curve for hits which are more than six standard deviations above noise. It can be seen that the plateau corresponds to $N_{pe} \approx 13$. This number has to be corrected for possible background hits, which we estimate to be about 1 per event. This performance is in close agreement with our expectations based on the performance of a similar prototype built and

tested by the College de France–Strasbourg group [7]. A tracking system is being added to this set-up to allow us to start measuring Cherenkov angular resolutions.

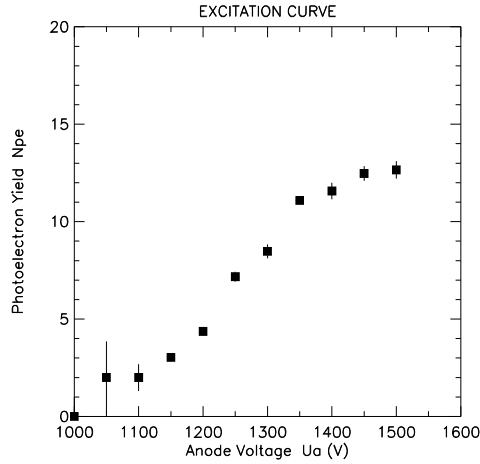


Figure 5: Excitation curve for CH₄-TEA. The voltage on the metallization of the CaF₂ windows is kept at -1350V.

5 Silicon vertex detector/tracker

In order to provide good measurements of angles and precise vertex positions, useful especially for charm decays, we are constructing a four layer double sided silicon device, which covers 93% of 4π . Our concept is to use only one detector size with $50\ \mu\text{m}$ strip pitch and external dimension of $2.7\text{cm} \times 5.26\text{cm} \times 300\ \mu\text{m}$.

The number of detectors and their properties are listed in Table 1. The large amount of capacitance on the fourth layer makes it difficult to achieve low noise performance. The noise target is $125e^- + 8e^-/\text{pf}$ in a radiation hard version of the chip. The rad-hard version of the Viking chip, VH1, gives $400e^- + 5e^-/\text{pf}$, which is almost good enough. The silicon group is pursuing making their own front end preamplifier.

The silicon electronic system is being developed along the same lines as the RICH electronics mentioned above. A possible system is outlined in Fig. 6.

Table 1: CLEO III silicon detector properties

| Layer# | r(cm) | # in ϕ | # in z | total # | C(pf) |
|--------|-------|-------------|--------|---------|-------|
| 1 | 2.4 | 7 | 4 | 28 | 12 |
| 2 | 3.8 | 10 | 4 | 40 | 19 |
| 3 | 7.5 | 20 | 8 | 160 | 38 |
| 4 | 12.0 | 30 | 12 | 360 | 60 |

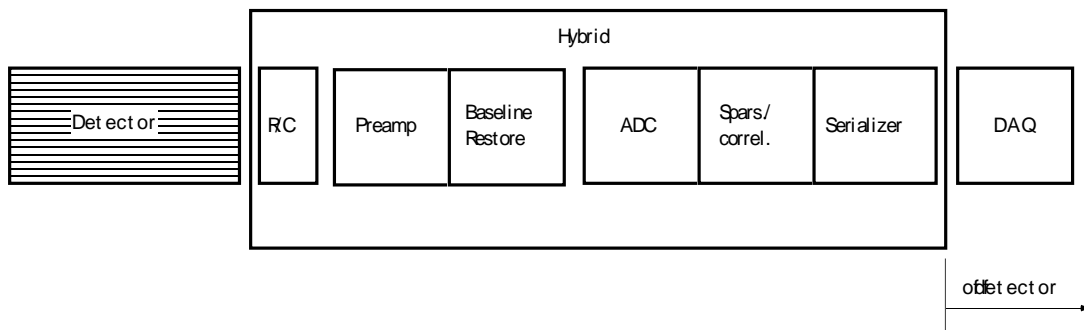


Figure 6: A view of the silicon electronics design outline. The bias resistors are off the detector.

6 Drift Chamber

In order to reduce multiple scattering which limits the tracking resolution, material in the chamber and the chamber walls is being reduced as much as possible. To help photon detection, the endplate is being constructed out of 1.5 cm thick shaped aluminum. To fit around the interaction region quadrupoles, there is an inner conical section which contains only axial wire layers and an outer cylindrical section which contains alternating stereo wire layers (see Fig. 2).

A Helium based gases will be used in the chamber. Properties of some of these gases are shown in Table 2 along with the “standard”, 50% Ar-50% CH₄ mixture. Here R_L is the radiation length, θ_L the Lorentz angle, #e/cm the number of ion pairs produced per cm, $\sigma(dE/dx)$ the resolution in the specific ionization measurement and e/π , the ratio of specific ionization between electrons and pions at minimum dE/dx loss. (The latter two quantities are from calculations.)

We have found spatial resolutions in test chambers of better than 100 μm for most of the

Table 2: Comparison of Drift Chamber gas properties

| Gas mixture | R_L | θ_L | #e/cm | $\sigma(dE/dx)$ | e/π |
|---|-------|------------|-------|-----------------|---------|
| Ar-C ₂ H ₆ (50:50) | 178 | 68.9 | 33.8 | 6.3% | 1.46 |
| He-C ₃ H ₈ (60:40) | 569 | 35.0 | 32.6 | 6.3% | 1.30 |
| He-C ₃ H ₈ (40:60) | 392 | 38.6 | 45.8 | 5.7% | 1.28 |
| He-C ₄ H ₁₀ (70:30) | 564 | 30.3 | 31.1 | 6.3% | 1.29 |
| He-C ₂ H ₆ (50:50) | 686 | 41.4 | 24.8 | 6.7% | 1.32 |

He based mixures, even when the test chambers have been placed in a 1.5T magnetic field. These resolutions are better than achieved in Ar-C₂H₆ in the same test setup. In Fig. 7 we show the hit efficiency for different gases as function of the incident track position across the drift cell. The efficiency is much better using the He based gases due to the smaller Lorentz angle. These gases are so promising that CLEO II will immediately adopt one of the He mixtures.

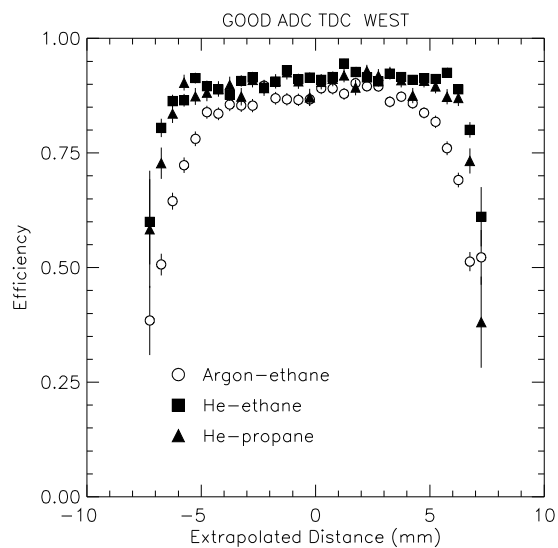


Figure 7: The hit efficiency across the drift cell for three different gases.

7 Acknowledgements

This work reported here is supported by the National Science Foundation. I thank M. Artuso, C. Bebek, H. Kagan and the RICH group at Syracuse Univ. for their help.

References

- [1] S. Stone, "Fundamental Constants from b and c Decay," HEPSY 94-5, in Proceedings of "Particle Strings and Cosmology," meeting, Syracuse, NY (1994), ed. K. Wali, World Scientific, Singapore (1995) and in "Proceedings of DPF94 Meeting," Albuquerque, NM (1994) ed. S. Seidel, World Scientific, Singapore (1995).
- [2] R. Ammar *et al.*, "Measurement of the Branching Ratios for exclusive $b \rightarrow ul\nu$ Decays," CLEO CONF 95/9, EPS0165 (1995).
- [3] D. Gibaut *et al.*, "Measurement of $\Gamma(D_s^+ \rightarrow \mu^+\nu)/\Gamma(D_s^+ \rightarrow \phi\pi^+)$," CLEO CONF 95-22, EPS0184 (1995).
- [4] S. Playfer and S. Stone, "Rare B Decays", HEPSY 95-01 (1995), to be published in Int. Journal of Mod. Phys. A.
- [5] Y. Kubota *et al.*, Nucl. Instr. and Meth. **A301**, **A320** (1992) 56.
- [6] J. Seguinot and T. Ypsilantis, Nucl. Instru. & Meth. **A343**, 1 (1994).
- [7] J.L. Guyonnet *et al.*, Nucl. Instr. & Meth. **A343** (1994) 178.
- [8] A. Efimov *et al.*, "Monte Carlo Studies of a Novel LiF Radiator for RICH Detectors," HEPSY 94-8 (1994), to be published in Nucl. Instr. & Meth.; M. Artuso, "The Ring Imaging Cherenkov Counter for CLEO III," presented at 6th Int. Symp. on Heavy Flavour Physics Pisa, Italy, June 1995, to appear in proceedings.
- [9] E. Nygard *et al.*, Nucl. Instr. and Meth. **A301** (1991) 506.
- [10] O. Milgrome *Talk given at the 2nd International Meeting on Front End Electronics for Tracking Detectors at Future High Luminosity Colliders* Perugia, Italy (1994); R. Yarema, "A Beginners Guide to the SVXII," FERMILAB-TM-1892 (1994).